



Study on the Effect of the Curvature of Solar Collector on Wind Loading Coefficients and Dynamic Response of Solar Collector

Aladine Abdulkader Kazem

Khalid Hameed Hussein

Department of Engineering Affair / University of Baghdad

(Received 4 February 2013; accepted 30 April 2013)

Abstract

In the current research, the work concentrated on studying the effect of curvature of solar parabolic trough solar collector on wind loading coefficients and dynamic response of solar collector. The response of collector to the aerodynamic loading was estimated numerically and experimentally. The curvature of most public parabolic trough solar collectors was investigated and compared. The dynamic response of solar collector due to wind loading was investigated by using numerical solution of fluid-structure interaction concept. The experimental work was done to verify the numerical results and shows good agreement with numerical results. The numerical results were obtained by using finite element software package (ANSYS 14). It was found that the change in collector curvature (focal length) lead to remarkable changes in wind loading coefficients (drag, lift, and moment), dynamic response (displacement) and natural frequencies but does not affect the first mode shape.

Keywords: *Solar collector, curvature, fluid-structure interaction and finite element.*

1. Introduction

The solar thermal power (STP) plants are used to concentrate the heat on the working substance used in steam production process for electrical generation. Solar thermal power plants are primarily installed in flat terrain of high solar irradiation for achieving a high power density [1]. The parabolic trough collector is considered to be the most suitable for concentration task [2]. At flat terrain, the components of plants are subjected to severe aerodynamic problems. The parabolic trough is the main component exposed to such aerodynamic effects. The main environmental problems which affect the parabolic trough performance are the wind-induced vibration and trough instability to track the sun accurately [3]. The study of dynamic response of solar collector due to environmental conditions is very useful to built suitable control system to adjust collector tracking system. The dynamic response of solar collector can be affected by many factors such as collector geometry, material, fixing, environmental conditions and the accuracy of

control system. This research aims to study the effect of the geometry of the collector on the dynamic response of the collector due to wind loading. M.T. Lates presents the finite elements analysis of the mechanical behavior for three main solar collector tracking systems: for plate, for dish and for trough solar collectors. The study concentrated on prediction of stresses in solar collectors due to extreme meteorological situations (3cm thick snow layer and 16m/s wind speed acting on the structure oriented at horizontal position [4]. A. Miliozzi et.al evaluated wind loads on a parabolic-trough concentrator numerically using the CFD Flotran module of Ansys finite element code. The study concentrated on evaluating the aerodynamics coefficient for the parabolic trough at three wind speed and different angular position [5]. L. M. murphy carried out a study to discuss the most practical designs for the collector and the test procedures to evaluate the wind loading on the collector. The test results corresponding to numerous wind tests on heliostats, parabolic troughs, parabolic dishes, and field mounted photovoltaic arrays are discussed and the applicability of the findings across the

various technologies is assessed [6]. J. A. Peterka et. al. carried out a study to define mean and peak wind loads on parabolic dish solar collectors. Loads on isolated collectors and on collectors within a field of collectors were obtained. A major intent of the study was to define wind load reduction factors for collectors within a field resulting from protection offered by upwind collectors, wind protective fences, or other blockage elements [7]. N. U. Gunasena performed a study to determine the feasibility of a novel solar collector design for large scale solar power generation. The design concept involved a large, fixed mirror dish in the shape of a spherical segment, with a tracking collector as opposed to a more traditional tracking concentrator with a fixed or tracking collector [8]. N. Hosoya and J.A. Peterka carried out comprehensive experimental study to determine the mean and maximum wind load coefficients on the parabolic trough in boundary layer wind tunnel. The wind loading on parabolic trough are determined for different angles of attack, for different wind speeds and for different turbulent intensity. This study showed that the wind loads coefficients are independent of the Reynolds number and turbulent intensity [9]. In this paper, the effect of geometry (curvature) of the parabolic trough solar collector on wind loading coefficients and wind-induced dynamic response of the collector was investigated. The wind loading coefficients included drag coefficient, lift coefficient, and moment coefficient. The dynamic response of collector which is studied in current study is the vibrational characteristics (natural frequency, mode shape and damping ratio) of the parabolic trough solar collector and the response (deformation) of the trough surface under the action of wind loading. Five scenarios of curvature of most public parabolic trough were considered and the dynamic response of all these scenarios under the action of one wind speed (10m/s) and one angle of attack ($\theta=90^\circ$) was investigated and compared.

2. Solar Collector Geometry

This paper specifically refers to parabolic trough collectors for concentrating sunlight. This type of concentrator has a cylindrical shape, with its parabolic curvature described by the formula ($Y=X^2/4f$). The distance (f) represents the position of the focal point of the parabola (the distance of the focal line of the parabola from its vertex). The difference in curvature leads to difference in length of aperture (d) and height (h).

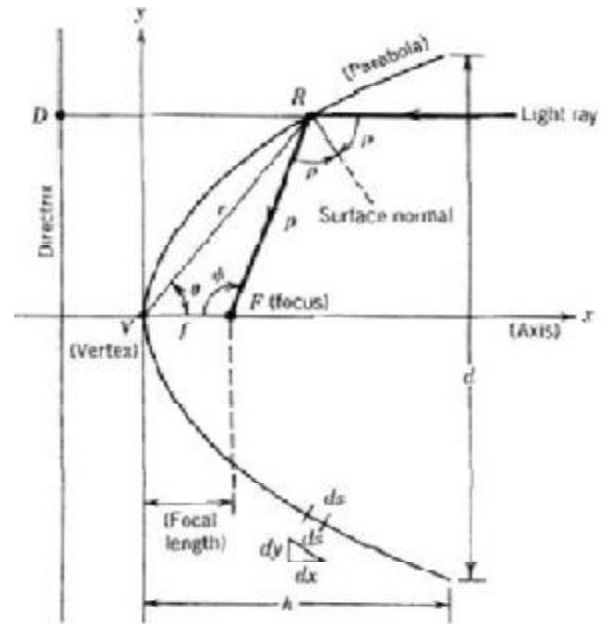


Fig. 1. Profile of the Present Parabolic Concentrator [10].

3. Scenarios of Curvature

Five of the most public parabolic trough curvatures were chosen for current study. The curvatures of these five types of collector are listed in Table (1) [11, 12 , 13]:

Table 1, Curvatures of Collectors.

Scenario	Collector	Focal length(m)	Parabola
S1	LS-1 ^[11,12]	0.94	$Y=X^2/3.7$ 6
S2	LS-2, Duke Solar ^[11,12]	1.49	$Y=X^2/5.9$ 6
S3	LS-3, Euro Trough ^[11,12]	1.71	$Y=X^2/6.8$ 4
S4	NEW IST ^[11,12]	0.76	$Y=X^2/3.0$ 4
S5	MIT-Trough ^[13]	0.1	$Y=X^2/0.4$

The investigation of the difference of dynamic response of different collectors due to wind loading requires the same aperture area for all collectors under the study. So, the aperture length (d) and the length of the parabolic trough must be the same for all prototypes. Therefore, the

difference between the collectors belongs to the difference in height (h). This difference in geometry will affect the flow characteristic distribution around the trough and subsequently will affect the dynamic response of the trough.

4. Numerical Simulation

ANSYS is a finite element analysis software package. In the current study, ANSYS workbench is used for fluid-structure interaction (FSI) analysis. FSI applications involve coupling of fluid dynamics and structure mechanics disciplines as in Figure (2) [14]:

- Fluid flow exerts hydrodynamic forces on a structure and deforms and/or translates the structure.
- Deformed or translated structure imparts displacement to the fluid domain and changes its shape and thus changes the fluid flow.

5. Modes of FSI Modeling

The main characteristics of modes of FSI modeling are listed in Table 2.

Table 2,
Comparison between Modes of FSI Modeling.

FSI simulation (1 way)	FSI simulation (2 way)
Very small deformations in the structure	Large structural deformations
Calculate and pass flow fields from CFD to the structural analysis FEA code	Iterate between CFD and FEA codes
No need to update and recalculate flow	need to update and recalculate flow

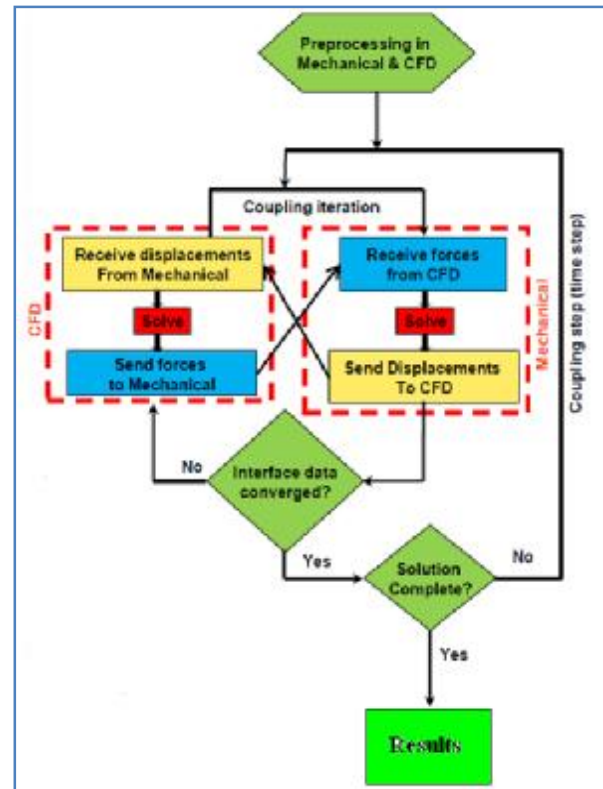


Fig. 2. Coupling Procedure of 2-way Fluid-Structure Interaction [14].

In the current paper, In current paper, both 1-way and 2-way fluid-structure simulation are done. For 1-way simulation, the (FLUENT ANSYS 14) version was used to evaluate the flow characteristics around the parabolic trough and the aerodynamic forces exerted by wind which was mapped to mechanical ANSYS to evaluate the response due to these aerodynamic forces. For 2-way simulation, The ANSYS 14 version was used with a FEM modeling facility for the trough structure and the CFX module for modeling the fluid flow. These two physics could be combined using the MFX multi-field solver. The key of the coupled simulation is that the fluid flow induces forces on the parabolic trough, which deforms accordingly based on the FEM calculations. The deformation was feed back to the CFD mesh.

6. Modal Analysis

The modal analysis is used to determine the vibration characteristics (natural frequencies and mode shapes) of the structure. It also can be a starting point for the harmonic response analysis. The basic equation solved in a typical modal analysis is the classical eigenvalue problem. Many

numerical methods are available to solve that equation.

7. Mesh Description

Two domains are used in numerical simulation, fluid domain and structure domain. The element used for structural analysis is (shell 281). The SHELL281 element is suitable for analyzing thin to moderately-thick shell structures. The element has eight nodes with six degrees of freedom at each node: translations in the x, y, and z axes, and rotations about the x, y, and z-axes. When using the membrane option, the element has translational degrees of freedom only [15]. This element is shown in Figure (3). Figure (4) shows the mesh density of the structure.

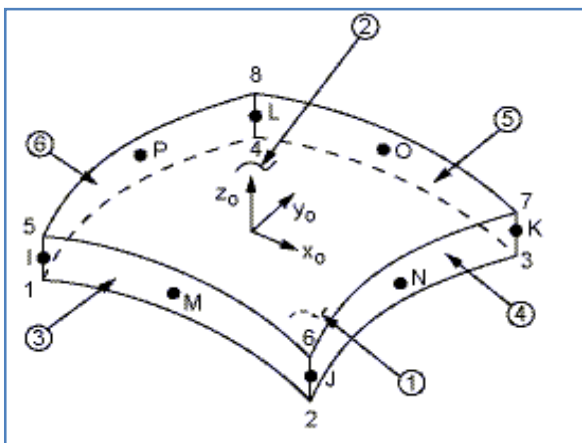


Fig. 3. Element Shell 281 Geometry. [15].

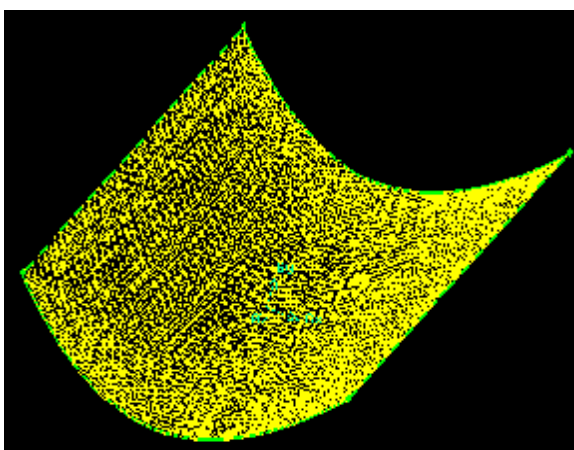


Fig. 4. Mesh of Structure.

For fluid domain, two types of elements were used. For a surface mesh, a higher order triangular element with hanging node was used as shown in

Figure (5-A) and for three dimensional mesh, higher order tetrahedral element with hanging nodes was used as shown in Figure (5-B). Figure (6) shows the mesh topology of fluid domain.

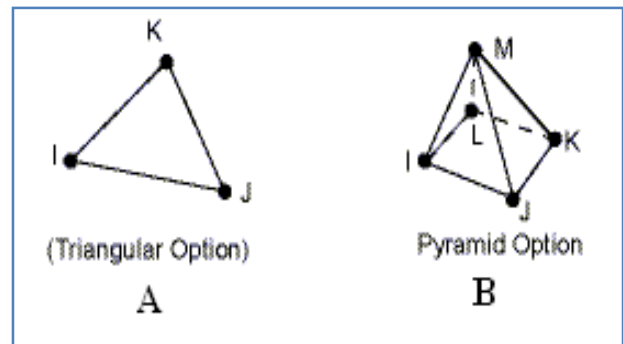


Fig. 5. Types of Elements of Fluid Domain [16].

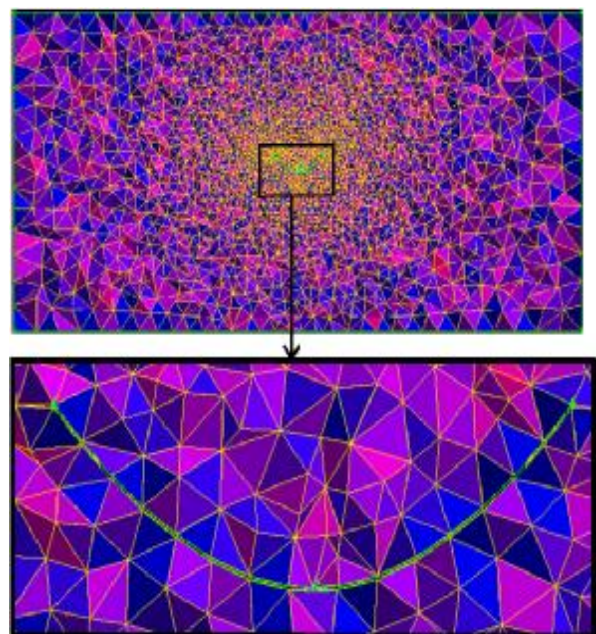


Fig. 6. The Mesh Topology of Fluid Domain.

8. Experimental Work

To verify the numerical results, an experimental work to measure the dynamic response of collector was done. The verification was done for one type of collector (MIT-Trough). The vibrational characteristics of the trough (natural frequencies and mode shape) were measured first. Then the dynamic response (displacement) under the action of wind loading was measured. One wind velocity (10m/s) and one angle of attack ($\theta = 90^\circ$) where the aperture is parallel to wind direction are used in current study.

9. Experimental Apparatus and Setup

The experimental work setups consist of dynamic response measurements (vibration behavior) and wind loading setup. The dynamic response measuring system consists of accelerometer, charge amplifier, oscilloscope and parabolic trough prototype. The schematic diagram of dynamic response measuring system is shown in Figure (7).

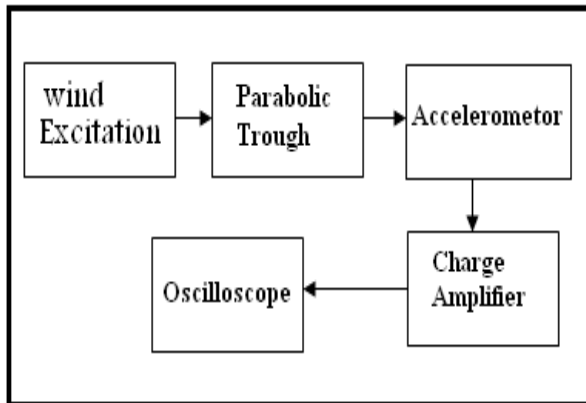


Fig. 7. Schematic Diagram of Response Measuring System.

The wind loading (pressure) measuring devices consist of several pressure tabs located on the surface of the trough. The system receive simultaneous signal samples from (8) individual pressure transducers at maximum design rate of (12500) samples per second per channel. The signals are transmitted from pressure transducers to (8) channels to analog to digital convertor serial communications USB (DAQmx 100 ksa/sec) connected to controller software (LabVIEW Signal Express 2010) on personal computer. This system allows digitizing, showing and saving the variations in pressure with time on Excel data sheet. The wind tunnel discharge is used as free jet to supply wind at different velocity. This free jet satisfies maximum wind velocity up to (24.6 m/s) at a distance 3m abroad from the free jet. The wind velocity was measured at many points at leeward edge of trough and the average value was calculated. The wind tunnel was adjusted to supply average wind velocity 10m/s at the leeward edge of trough. The velocity of wind is measured by using calibrated flow meter.

10. Parabolic Trough Setup

One type of parabolic trough was used in experimental work to examine the validity of using the numerical simulation. The prototype used in this study is made from composite material (polyester resin and E-glass fibers). It is fabricated by using special mold installed for this purpose. The surfaces of trough are polished. The surfaces are smoothed using different wet silicon carbide starting with (260) to (1200) for finishing and then polished using polishing cloth and alumina. The final step is the washing of product by using distilled water for 10 minutes. The final product with dynamic response measuring system is shown in figure (8). The manufacturing processes and the mixing percentage were chosen according to ASM Metal Handbook standard for composite [17].



Fig. 8. The Parabolic Trough Made from Composite Material.

11. Result and Discussion

The results of the current research are divided into three categories: the verification of numerical result, the effect of the curvature on wind loading coefficients and the effect of the curvature on the dynamic response of the collector.

12. Verification of Numerical Results

The verification of the numerical results included the verification of flow characteristic and the verification of dynamic response of the parabolic trough.

1. Flow characteristics verification: The experimental data of two parameters were used in

this verification. The first was the experimental data of static pressure distribution over the parabolic trough and the second parameter was the wind loads coefficients on the parabolic trough. The values of static pressure at specific points on the trough surface were measured experimentally and the counter of pressure over trough surface was drawn and then compared with contour of static pressure which is obtained from numerical work. Figures (9 and 10) show these contours of pressure. In both figures the high values of pressure are appears near the edges of trough. Also, both experimental and numerical analysis shows that the values of pressure are approximately symmetrical around the centerline of trough. In experimental work, the minimum value of static pressure was 20pa and the maximum value was 70pa while in numerical analysis the minimum value of static pressure was 14.3pa and the maximum value was 71.5pa. It is clear from these figures that the numerical results show good agreement with experimental results. The wind loading coefficients (drag, lift, and moment) are obtained experimentally by using rigid model. This model designed to measure the distribution of local pressures on the front surface of the rigid collector concentrator module. Distribution of point pressures can be integrated over the parabolic concentrator surface to numerically determine the total loads on the parabolic trough solar collector. The formula of calculating these coefficients are shown in Appendix (1). Also, these loading coefficients are obtained numerically. The values of these coefficients are listed in Table (3). It is clear from these results that the numerical simulation of the wind loading gives excellent coincides with experimental results.

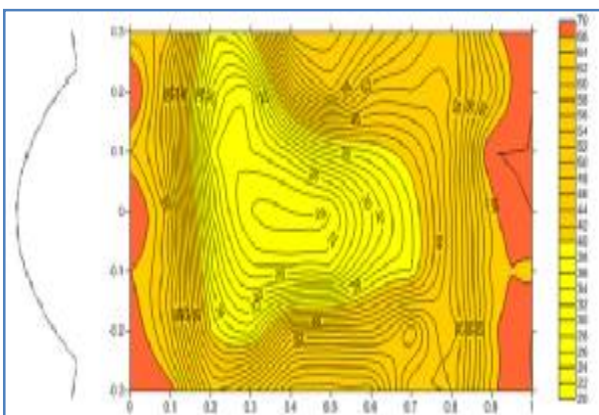


Fig. 9. Contours of Static Pressure Over Trough Surface at Wind Velocity 10m/s Obtained from Experimental Work.

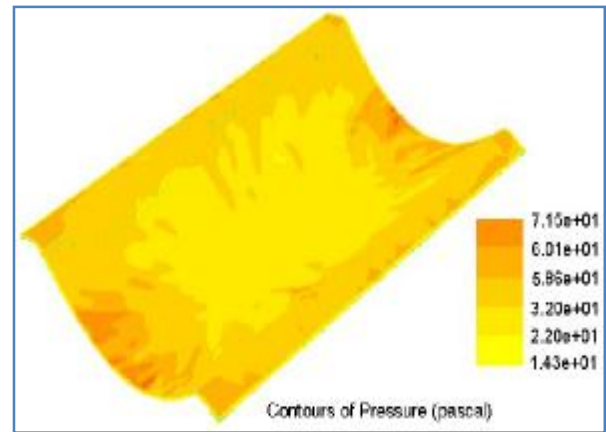


Fig. 10. Contours of Static Pressure Over Trough Surface at Wind Velocity 10m/s Obtained from Numerical Analysis.

Table 3, Wind Load Coefficients of MIT Trough at Velocity 10m/s

	Drag coefficient	Lift coefficient	Moment coefficient
Experimental	0.395	-0.232	0.637
Numerical	0.432	-0.214	0.613
Error %	9.367	-7.758	-3.767

2. Dynamic response verification: The displacement at specific point on trough surface was measured while the wind is applied on trough surface. Also, the displacement of the same was evaluated numerically. Figure (11) shows the comparison between these results. The comparison between experimental and numerical results of dynamic response shows that the experimental results always larger than the numerical results but the differences were within acceptable range. This difference appears because the actual structure has flexibility more than the numerical model. The numerical results of wind induced response of parabolic trough show that the results of 2-way fluid-structure simulation are close to 1-way simulation. This can be attributed that the response of trough due to this wind velocity was very small and did not alter the flow around the trough.

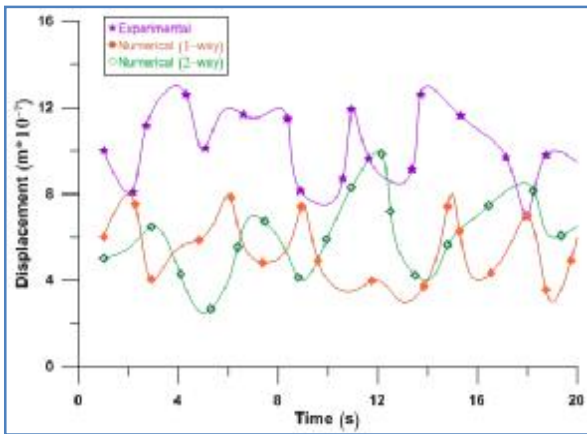


Fig. 11. Dynamic Response of a Point Parabolic Trough Surface.

13. The Effect of the Curvature on Wind Loading Coefficients

The flow characteristics and dynamic response of one type of collector (MIT collector) are estimated experimentally and numerically. The results show good agreement between them. So, the numerical simulation then used to estimate the flow characteristic and dynamic response of other types of collector and make a comparison between them to find the effect of the curvature on the results. Table (4) lists the wind loading coefficients for all types of collectors at wind velocity 10m/s and angle of attack ($\theta=90^\circ$). It is shown that the drag coefficient increases with the decreasing of focal length. This can be attributed that the decreasing of focal length leads to increasing of side projected area of the trough. This situation will inverse when lift coefficient is considered where the decreasing of focal length leads to decreasing of lift coefficient because that the top projected area will decreased. The difference in moment coefficient is more complicated than the difference in drag and lifts coefficients where the moment is the result of drag force moment and lift force moment. For parabolic trough, the increasing of focal length leads to decreasing the moment coefficient. This indicates that the changing of the curvature of the parabolic trough has more effect on the drag force than that on lift force. Figure (12) shows the comparison between the wind loading coefficients. It is clear that the (MIT collector) has the highest value of drag and moment coefficients whereas the (Euro trough and LS-3 collectors) has the minimum value of drag and moment coefficients. The minus sign of lift coefficient indicates that the lift force directed into downward

because of the concave of the trough at this angle of attack. The highest value of lift coefficient was recorded for (Euro trough and LS-3 collectors) and the lowest value was recorded for (MIT trough).

Table 4, Wind Loading Coefficients For All Types of Collector.

scenario	Drag coefficient	Lift coefficient	Moment coefficient
S1	0.385	-0.267	0.554
S2	0.321	-0.294	0.531
S3	0.303	-0.312	0.501
S4	0.402	-0.235	0.571
S5	0.432	-0.214	0.613

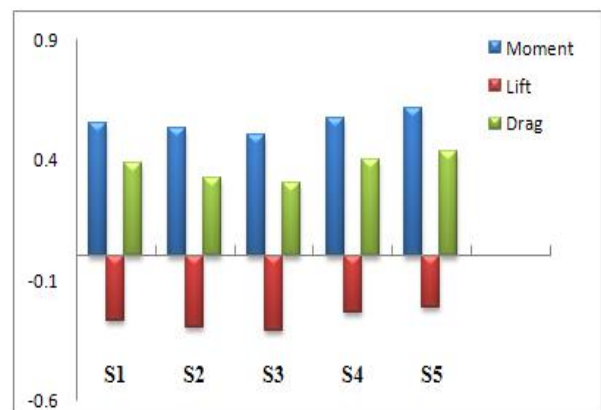


Fig. 12. Comparison between the Wind Loading Coefficients.

14. The Effect of Curvature on Dynamic Response of Collector

The dynamic response included the natural frequencies, mode shape and displacement due to wind loading. Table (5) lists the values of first three natural frequencies of all types of collector and Figure (13) shows the comparison between these values. It is obvious from this figure that the values of natural frequencies increase with the decreasing of focal length. This can be attributed to the effect of rigidity of shell structure. The more curvature leads to more rigidity and this leads to increasing the value of natural frequency. The natural frequencies of (MIT) collector were higher than the natural frequencies of other types and the increment from first natural frequency to second and from second to third are very large in

comparison with the other types. This increment is very little for scenarios (S1, S2 and S3). The presence of folded edges in (MIT) collector leads to increasing the values of natural frequency. The values of natural frequencies of scenarios (S2 and S3) are close because the focal lengths are close.

Table 5,
The First Three Natural Frequencies of all types of Solar Collector.

Scenario	First natural frequency (Hz)	Second natural frequency (Hz)	Third natural frequency (Hz)
S1	41.54	48.443	51.84
S2	29.563	32.854	37.54
S3	25.74	26.4	28.548
S4	44.56	56.3	56.768
S5	75.016	83.324	134.74

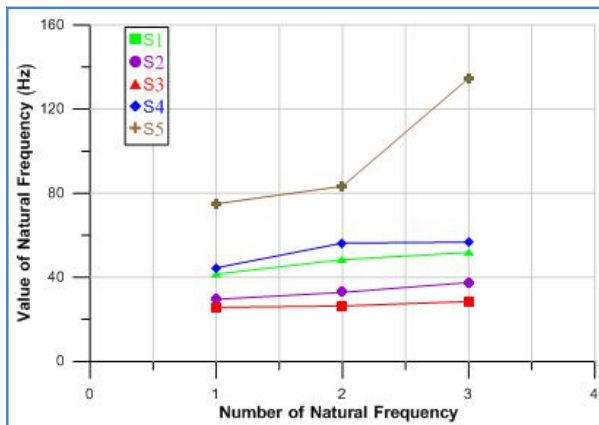


Fig. 13. Comparison between the Natural Frequencies of all Types of Collectors.

The numerical estimation of mode shapes shows that the first mode shape is the same for all types of collector. This similarity is caused because that the mode shape depends in very high proportion on the boundary condition and the type of excitation. The difference in focal length does not lead to high changes in the first mode shape. Figure (14) shows the first mode shape of all types the collectors. Appendix (2) shows the first, second and third mode shape of (MIT) collector.

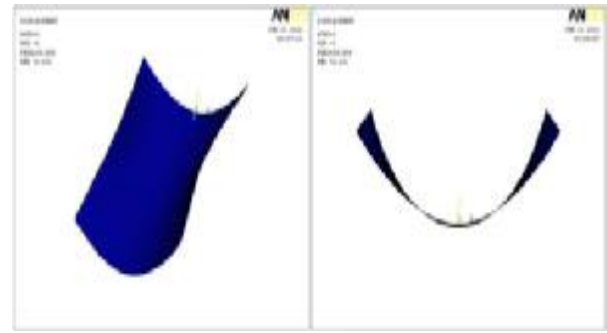


Fig. 14. First Mode Shape of the Collectors.

The responses (displacement) of solar collectors due to wind loadings are evaluated numerically by using 1-way and 2-way FSI to estimate the effect of the curvature on displacement response of collectors. Only the results of 2-way FSI will present because the results of 1-way are close to 2-way results as shown in figure (11). Figure (17) show the comparison between the dynamic responses of all types of collectors. It is clear from this figure that the displacement of a point on collector surface due to wind loading increases with the increasing of focal length because that the flexibility of collector surface increase with the increasing of focal length. Also, it is clear that the scenario (S5) has the highest rigidity between all scenarios. This can be attributed to the presence of folded edges. The changes of displacement are random with time. This indicate that the wind loading excite the collector to vibrate in compound mode of vibration because the wind loading is also random and consist of a spectrum of frequencies. Although, the values of displacement are seems to be very small because the wind loading at this wind velocity (10m/s) is not sufficient to excite the collector with high level of response.

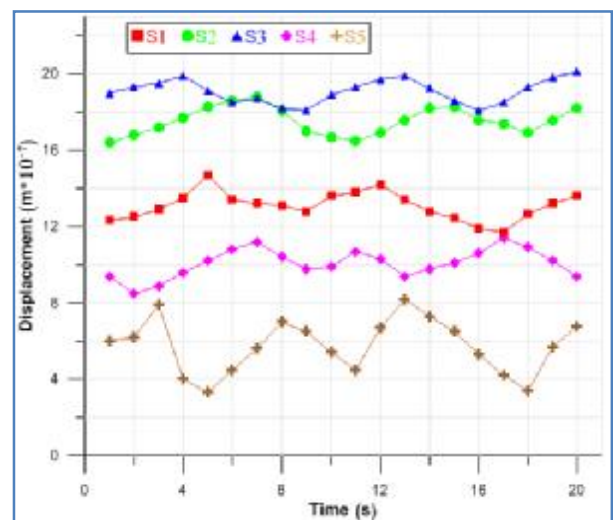


Fig. 15. Displacement of Collectors due to Wind Loading.

15. Conclusion

The most important conclusions drawn from this research are:

- 1- The drag coefficient increases with the decreasing of focal length because the decreasing of focal length leads to increasing vertical projected area and this will increase the friction part of drag.
- 2- Decreasing of focal length leads to decreasing of lift coefficient because the decreasing of focal length leads to decreasing the horizontal projected area.
- 3- The increasing of focal length leads to decreasing the moment coefficient.
- 4- Changing of the curvature of the parabolic trough has more effect on the drag force than that on lift force because the drag force depend on pressure drag and friction drag and the changing the projected area leads to changing in flow pattern around the collector where the friction drag will increase significantly.
- 5- The values of natural frequencies increase with the decreasing of focal length because the rigidity of the collector will increase.
- 6- The difference in focal length does not lead to high changes in the first mode shape.

- 7- The displacement of a point on collector surface due to wind loading increases with the increasing of focal length because the rigidity of the collector will decrease.

16. Appendix 1: Load Coefficients [9]

Wind load effects are characterized in terms of non-dimensional coefficients. The definitions of the load coefficients are:

$$\text{Drag horizontal Force coefficient} \quad cf_x = \frac{f_x}{qLd}$$

$$\text{Lift vertical Force coefficient} \quad cf_z = \frac{f_z}{qLd}$$

Pitching Moment coefficient

$$Cm_y = \frac{M_y}{qLd^2}$$

Where f_x , f_z , and M_y are the aerodynamic loads. These aerodynamics loads are calculated by integrating the point pressure values over the trough surface. L is the length of the trough, and d is the aperture width of the collector Figure (1). The quantity, q , is the mean reference dynamic pressure measured at the height of the solar collector.

$q = \frac{1}{2} \rho U^2$ Here U is the mean wind speed at the height, and ρ is the density of air.

17. Appendix 2: The First, Second and Third Mode Shape of MIT Collector

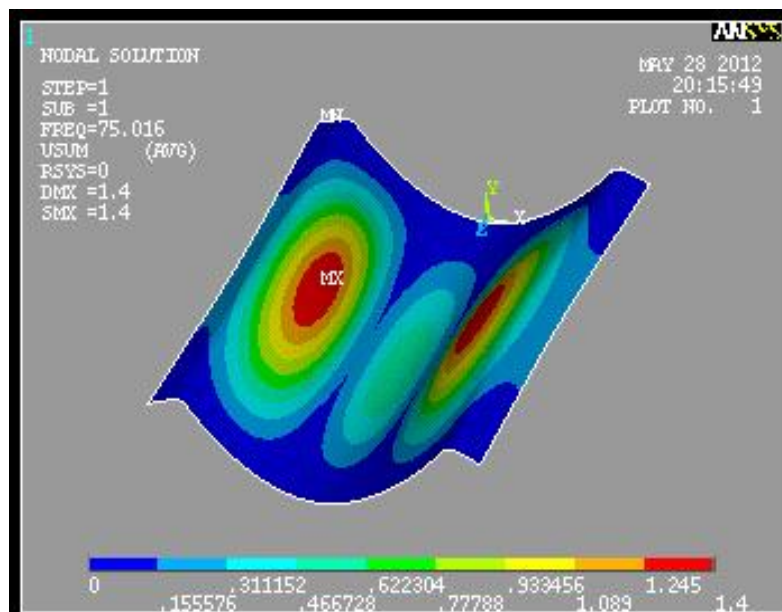


Fig. 16. First Mode Shape.

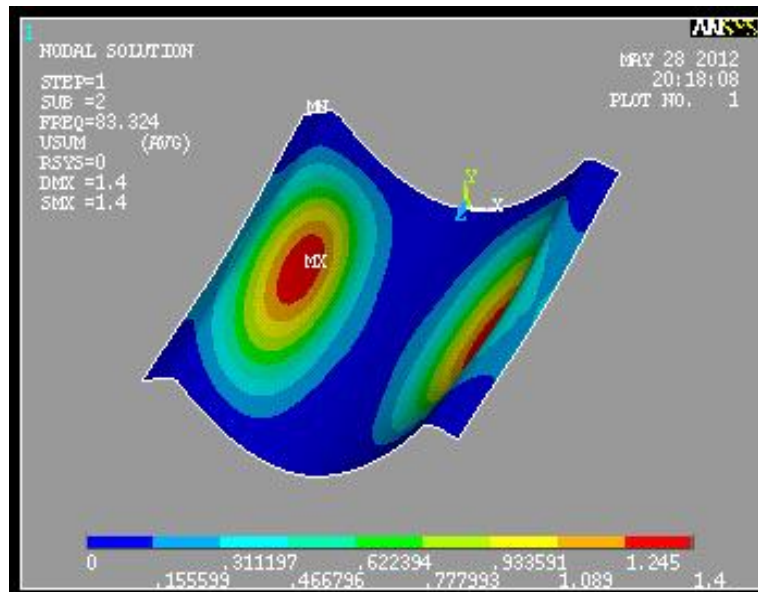


Fig. 17. Second Mode Shape.

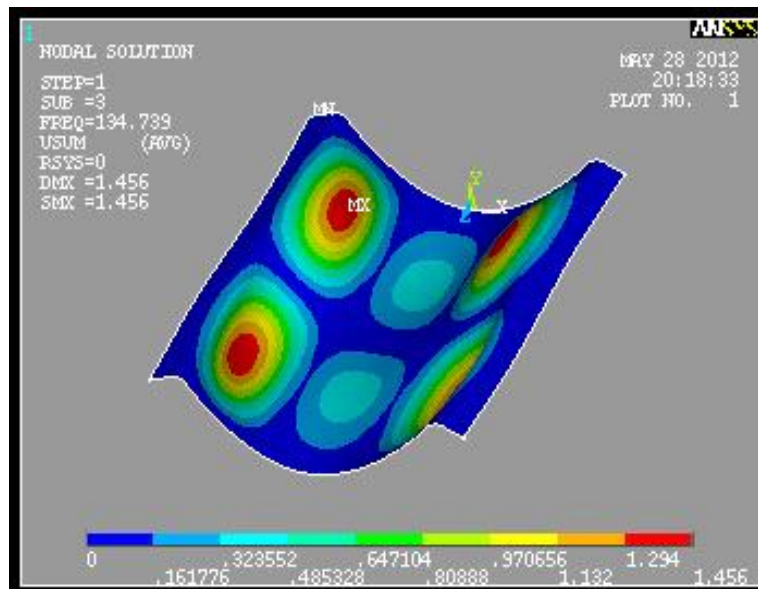


Fig. 18. Third Mode Shape

18. References

- [1] H. H. Hamad, "Study on wind loads coefficients and flow field characteristics around the parabolic trough with stiffeners" University of Technology, Baghdad, 2012.
- [2] Soteris A. Kalogirou " Solar thermal collectors and applications" Progress in Energy and Combustion Science, 30 (2004), 231–295.
- [3] N. Naeni, M. Yaghoubi, "Analysis of wind flow around a parabolic collector" Renewable Energy 32 (2007) 1898–1916.
- [4] M.T. Lates, Mechanical Behavior Analysis with the Finite Element Method of Solar Collectors Tracking Systems. Wseas transaction on applied and theoretical mechanics. Issn 1991-8747, issue 7, volume 3, July 2008.
- [5] A. Miliozzi, D. Nicolini, G. Arsuffi and L. Sipione. Numerical evaluation of Wind action on Parabolic Trough Collectors. 8th. World Congress on Computational Mechanics (WCCM8). 2008.
- [6] L.M. morphy, "wind loading on tracking and field mounted solar collectors", Solar energy research institute, Golden, Colorado, 80401, 1980.
- [7] J.A.peterka, Z. Tan, B. Bienkiwicz, J. E. Cermak, Fort Collins, "Wind Loads on

- Heliostats and Parabolic Dish Collectors”, Solar energy research institute, 1988.
- [8] N. U. Gunasena, “An experimental study of mean wind forces on hemispherical solar collectors”, M.Sc thesis, Texas tech university, 1989.
- [9] N. Hosoya and J.A. Peterka, “wind tunnel tests of parabolic trough solar collector”, National renewable energy laboratory, 2008.
- [10] Zeinab S. Abdel-Rehim, Ashraf Lasheen, “Experimental and theoretical study of a solar desalination system located in Cairo, Egypt”, Science direct, Desalination 217 (2007) 52–64.
- [11] Eckhard Lüpfert, Michael Geyer, Wolfgang Schiel, Antonio Esteban, Rafael Osuna, Eduardo Zarza, Paul Nava “Eurotrough design issues and prototype testing at PSA”, Proc. of ASME Int. Solar Energy Conf.-Forum 2001, Solar Energy: The Power to Choose, Washington, DC, April 21-25, pp. 389–394.
- [12] Hank Price, Eckhard Lüpfert, David Kearney, Eduardo Zarza, Gilbert Cohen, Randy Gee, “Advances in Parabolic Trough Solar Power Technology”, Journal of Solar Energy Engineering, MAY 2002, Vol. 124 / 109
- [13] Stacy L. Figueredo, Parabolic Trough Solar Collectors: Design for Increasing Efficiency, Ph.D thesis, Mechanical engineering department, MIT, 2011.
- [14] H. H. Hamad, “Dynamic response of solar concentrating power system for self cleaning”, Ph.D. thesis, University of Technology, Mechanical Engineering department, 2012.
- [15] ANSYS theory reference. Twelve edition, 2009, ANSYS Inc., South Point, Canonsburg, 2004.
- [16] - Sinan. A. Ali “ Study effect of Riblet Upstream Wing-Wall junction Numerically and Experimentally” ,M.Sc. thesis, Mechanical eng. Dept. University of Technology, 2011.
- [17] ASM Handbook, Volume 21, composite, 2001.

دراسة تأثير انحناء المجمع الشمسي على الاستجابة الديناميكية للمجمع الشمسي

علاء الدين عبد القادر خالد حميد حسين

قسم الشؤون الهندسية / جامعة بغداد

الخلاصة

في هذا البحث، تركز العمل على دراسة تأثير انحناء المجمع الشمسي ذو المقطع بشكل قطع مكافئ على معاملات الاحمال الهوائية والاستجابة الديناميكية للمجمع الشمسي. تم ايجاد استجابة المجمع لتأثير الاحمال الهوائية عدديا وعمليا. تمت دراسة انحناء اكثر المجمعات الشمسية استخداما في العالم وتمت المقارنة بينها. تمت دراسة الاستجابة الديناميكية للمجمع الشمسي باستخدام الحل العددي لمفهوم تفاعل المائع-الهيكل. تم اجراء الجانب العملي للتحقق من دقة النتائج العددية وقد اظهرت النتائج العملية تقاربا جيدا مع النتائج العملية. النتائج العددية استخرجت باستخدام طريقة العناصر المحددة عن طريق برنامج المحاكاة الحاسوبي ANSYS 14. لقد وجد ان تغيير تقوس المجمع الشمسي (البعد البؤري) ادى الى تغيرات واضحة في قيمة الاحمال الهوائية (الكبح، الرفع والعزم)، الاستجابة الديناميكية (الازاحة) وكذلك الترددات الطبيعية ولكن نسق الاهتزاز الاول لم يتأثر.